



ISSN: 0067-2904

Study of Matter Density Distributions, Elastic Electron Scattering Form factors and Root Mean Square Radii of ${}^9\text{C}$, ${}^{12}\text{N}$, ${}^{23}\text{Al}$, ${}^{11}\text{Be}$ and ${}^{15}\text{C}$ Exotic Nuclei

Shaimaa A. Rahi*, Ghaith N. Flaiyh

Department of Physics, College of Science, University of Baghdad, Baghdad, Iraq

Received: 1/5/2021

Accepted: 9/8/2021

Abstract:

The ground state densities of neutron-rich (${}^{11}\text{Be}$, ${}^{15}\text{C}$) and proton-rich (${}^9\text{C}$, ${}^{12}\text{N}$, ${}^{23}\text{Al}$) exotic nuclei are investigated using a two-body nucleon density distribution (2BNDD) with two frequency shells model (TFSM). The structure of the valence one-neutron of ${}^{11}\text{Be}$ is in pure ($1p_{1/2}$) and of ${}^{15}\text{C}$ in pure ($1d_{5/2}$) configuration, while the structure of valence one-proton configuration is in ${}^9\text{C}$, ${}^{12}\text{N}$ are to be in a pure ($1p_{1/2}$) and ${}^{23}\text{Al}$ in a pure ($2s_{1/2}$). For our studied nuclei, an efficient (2BNDD) operator for point nucleon system folded with two-body correlation operator's functions is used to investigate nuclear matter density distributions, elastic electron scattering form factors, and root-mean square (rms) radii. The effect of the strong tensor force (TC) in nucleon-nucleon forces is taken into account in the correlation. The wave functions of a single particle harmonic oscillator are used with two different oscillator size parameters, β_c and β_v , the former for core (inner) orbits and the latter for valence (halo) orbits. The measured matter density distributions of these nuclei clearly show the long tail results. The plane wave born approximation (PWBA) is used to investigate the elastic electron scattering form factors for these exotic nuclei.

Keywords: exotic nuclei, nucleon density distribution (2BNDD's), elastic electron scattering form factors, root-mean square (rms) radii, two-body correlation operator's functions.

دراسة كثافة توزيع المادة والاستطارة الالكترونية ومربع نصف القطر لبعض النوى الغريبة

(${}^9\text{C}$, ${}^{12}\text{N}$, ${}^{23}\text{Al}$, ${}^{11}\text{Be}$, ${}^{15}\text{C}$)

شيماء علي راهي*, غيث نعمة فليح
قسم الفيزياء، كلية العلوم، جامعة بغداد، بغداد، العراق

الخلاصة

تمت دراسة توزيعات الكثافة لبعض النوى الغريبة الغنية بالنيوترونات (${}^{11}\text{Be}$, ${}^{15}\text{C}$) والغنية بالبروتونات (${}^9\text{C}$, ${}^{12}\text{N}$, ${}^{23}\text{Al}$) من خلال دالة التوزيع للنكليونات ذو صيغة الجسيمين (2BNDD's) مع نموذج القشرة ثنائي التردد. اوضحت هذه الدراسة ان النيوكليون الفعال للنوى الغنية بالنيوترونات له التشكيل النقي عند ($1p_{1/2}$) لنواة ${}^{11}\text{Be}$ و ($1d_{5/2}$) لنواة ${}^{15}\text{C}$, وكذلك النيوكليون الفعال للنوى الغنية بالبروتونات له تشكيل نقي عند ($1p_{1/2}$) للنوى ${}^9\text{C}$, ${}^{12}\text{N}$ و ($2s_{1/2}$) لنواة ${}^{23}\text{Al}$. ان كثافة توزيعات المادة، عوامل التشكل المرنة للالكترونات

*Email: shimaa.rahi1204@sc.uobaghdad.edu.iq

المستطار وجذر مربع نصف القطر تمت دراستها للنوى قيد الدراسة من خلال المؤثر الفعال ذو صيغة الجسيمين مع الاخذ بنظر الاعتبار وجود مؤثر القوة التنزورية بين نيوكليون-نيوكليون. استخدمت الدالة الموجية لجهد المتذبذب التوافقي البسيط مع قيمتين مختلفتين للمتذبذب βC لنواة القلب و βv للنيكلونات خارج القلب. تم الحصول على سلوك الذيل الطويل في حسابات كثافة توزيعات النيوكلون للنوى قيد الدراسة. لوحظ ظاهرة الذيل الطويل بوضوح في توزيعات كثافة المادة للنوى المدروسة . عوامل التشكل للاستطارة الالكترونية المرنة لهذه النوى الغريبة تم دراستها باستخدام تقريب بورن للموجة المستوية .

Introduction:

Since the structure and decay modes of several nuclei far from stability are still unknown, exotic nuclei research is one of the most exciting research areas of modern nuclear physics[1]. It has become a challenging topic in nuclear physics since the discovery of neutron halo phenomena in ^{11}Li [2]. Weak binding energies describe the proton-and neutron-rich regimes in the nuclei chart, resulting in "exotic" features known as halos. [3].

Exotic nuclei are distinguished by the fact that they are far from the stability valley and have an abnormal N/Z ratio, implying that they have more protons or neutrons than stable nuclei; thus, these nuclei are referred to as proton-rich nuclei or neutron-rich nuclei. Matter density distribution $\rho_m(r)$ of a nucleus is essential to describe the nuclear structure. This fascination with $\rho_m(r)$ stems from fundamental bulk nuclear properties such as nuclei shape and size, binding energies, and other quantities linked to $\rho_m(r)$. Experimental matter density distributions of exotic nuclei are mainly characterized by long tail behavior at large r [4]. The inclusion of strong tensor force is one of the most fundamental nuclear forces, but its first-order effect on the shell structure has been clarified only recently in studies on exotic nuclei. The tensor force can change the spin-orbit splitting depending on the occupation of specific orbits[5]

The two-frequency shell model (TFSM) and the binary cluster model (BCM) are used to investigate the ground state densities of unstable proton-rich ^9C , ^{12}N , and ^{23}Al exotic nuclei [6]. A simple phenomenological method for introducing dynamical short range and tensor correlations was presented by Dellagiaco et al. [7]. Two versions of the density distribution of the one-proton halo ^{17}F nucleus have been taken into account in order to derive the double folding potentials. The measured angular distributions of elastic scattering differential cross section and the corresponding reaction cross sections have been successfully reproduced at different energies using the derived potentials[8]. Sultan [9] has used the binary cluster model BCM to investigate neutron, proton, and matter densities in the ground state of the exotic ^{14}B and ^{17}C nuclei.

Theory:

The one body density operator can be transformed into a two-body density form by the following transformation [10]:

$$\hat{\rho}^{(1)}(\vec{r}) = \sum_{i=1}^A \delta(\vec{r} - \vec{r}_i) \quad (1)$$

$$\hat{\rho}^{(1)}(\vec{r}) \Rightarrow \hat{\rho}^{(2)}(\vec{r})$$

i.e

$$\sum_{i=1}^A \delta(\vec{r} - \vec{r}_i) \equiv \frac{1}{2(A-1)} \sum_{i \neq j} \left\{ \delta(\vec{r} - \vec{r}_i) + \delta(\vec{r} - \vec{r}_j) \right\} \quad (2)$$

In fact, a further useful transformation can be made which is that the coordinates of the two – particles, \vec{r}_i and \vec{r}_j , be in terms of the relative \vec{r}_{ij} and center – of – mass \vec{R}_{ij} coordinates [11].

$$\vec{r}_{ij} = \frac{1}{\sqrt{2}}(\vec{r}_i - \vec{r}_j) \tag{3a}$$

$$\vec{R}_{ij} = \frac{1}{\sqrt{2}}(\vec{r}_i + \vec{r}_j) \tag{3b}$$

Subtracting and adding Eq. (3a) and Eq. (3b) the following relations can be obtain:

$$\vec{r}_i = \frac{1}{\sqrt{2}}(\vec{R}_{ij} + \vec{r}_{ij}) \tag{3c}$$

$$\vec{r}_j = \frac{1}{\sqrt{2}}(\vec{R}_{ij} - \vec{r}_{ij}) \tag{3d}$$

Introducing Eq. (3c) and (3d) into Eq. (2) yields:

$$\hat{\rho}^{(2)}(\vec{r}) = \frac{\sqrt{2}}{(A-1)} \sum_{i \neq j} \left\{ \delta \left[\sqrt{2} \vec{r} - \vec{R}_{ij} - \vec{r}_{ij} \right] + \delta \left[\sqrt{2} \vec{r} - \vec{R}_{ij} + \vec{r}_{ij} \right] \right\} \tag{4}$$

Finally, an effective two-body nucleon density operator (to be used with uncorrelated wave functions) can be produced by folding the operator of Eq.(4) with the two-body correlation functions \tilde{f}_{ij} as :

$$\hat{\rho}_{eff}^{(2)}(\vec{r}) = \frac{\sqrt{2}}{2(A-1)} \sum_{i \neq j} \tilde{f}_{ij} \left\{ \delta \left[\sqrt{2} \vec{r} - \vec{R}_{ij} - \vec{r}_{ij} \right] + \delta \left[\sqrt{2} \vec{r} - \vec{R}_{ij} + \vec{r}_{ij} \right] \right\} \tilde{f}_{ij} \tag{5}$$

In this work , a simple model form of the two-body tensor correlation operators used by fiase et al. [12] was adopted, i.e

$$\tilde{f}_{ij} = \left\{ 1 + \alpha(A) S_{ij} \right\} \Delta_2 \tag{6}$$

The two-body tensor correlations (TC) presented in Eq.(6) are induced by the strong tensor component in the nucleon- nucleon force and they are of longer range. Here Δ_2 is a projection operator onto the 3S_1 and 3D_1 states only. However, Eq. (6) can be rewritten as :

$$\tilde{f}_{ij} = \sum_{\gamma} \left\{ 1 + \alpha_{\gamma}(A) S_{ij} \right\} \Delta_{\gamma} \tag{7}$$

where the sum γ , in Eq.(7), is overall reaction channels, S_{ij} is the usual tensor operator, formed by the scalar product of a second-rank operator in intrinsic spin space and coordinate space and is defined by

$$S_{ij} = \frac{3}{r_{ij}^2} (\vec{\sigma}_i \cdot \vec{r}_{ij})(\vec{\sigma}_j \cdot \vec{r}_{ij}) - \vec{\sigma}_i \cdot \vec{\sigma}_j \tag{8}$$

while $\alpha_{\gamma}(A)$ is the strength of tensor correlations and it is non zero only in the $^3S_1 - ^3D_1$ channels.

As the halo nuclei is oversized and easily broken system consisting of a compact core plus a number of outer nucleons loosely bound and specially extended far from the core, it is suitable to separate the ground state density distribution of Eq. (5) into two parts, one is

connected with the core nucleons and the other with the halo nucleons, so matter density distribution for the whole halo nucleus becomes [13]:

$$\rho_m(r) = \rho_{p+n}^{core}(r) + \rho_{p(n)}^{valance}(r) \quad (9)$$

The normalization condition of the above ground state densities is given by:

$$g = 4\pi \int_0^{\infty} \rho_g(r) r^2 dr \quad (10)$$

Here $\rho_g(r)$ represents one of the following densities: matter, charge, core, or halo densities. The rms radii of corresponding above densities are given by:

$$\langle r \rangle_g^{1/2} = \frac{4\pi}{g} \int_0^{\infty} \rho_g(r) r^4 dr \quad (11)$$

Elastic electron scattering form factor from spin zero nuclei ($J=0$), can be determined by the ground – state charge density distributions (CDD). In the Plane Wave Born Approximation (PWBA), the incident and scattered electron waves are considered as plane waves and the CDD is real and with spherical symmetry, therefore the form factor is simply the Fourier transform of the CDD. Thus [14,15]

$$F(q) = \frac{4\pi}{qZ} \int_0^{\infty} \rho_o(r) \sin(qr) r dr F_{fs}(q) F_{cm}(q) \quad (12)$$

where $F_{fs}(q)$ is the finite nucleon size and $F_{cm}(q)$ the center of mass corrections. $F_{fs}(q)$ is considered as free nucleon form factor and assumed to be the same for protons and neutrons. This correction takes the form [15]:

$$F_{fs}(q) = e^{-0.43q^2/4} \quad (13)$$

The correction $F_{cm}(q)$ removes the spurious state arising from the motion of the center of mass when shell model wave function is used and is given by [14]:

$$F_{cm}(q) = e^{q^2 b^2 / 4A} \quad (14)$$

Where A is the nuclear mass number.

Results and Discussion:

The nuclear ground state properties of one-neutron (^{11}Be , ^{15}C) and one-proton (^9C , ^{12}N , ^{23}Al) exotic nuclei have been calculated using 2BNDD including the effect of two-body tensor correlations (TC) using two frequency shell model (TFSM). The calculations were based on using different model spaces for the core and the extra halo nucleon. The single particle harmonic oscillator wave functions were employed with two different size parameters of β_c and β_v .

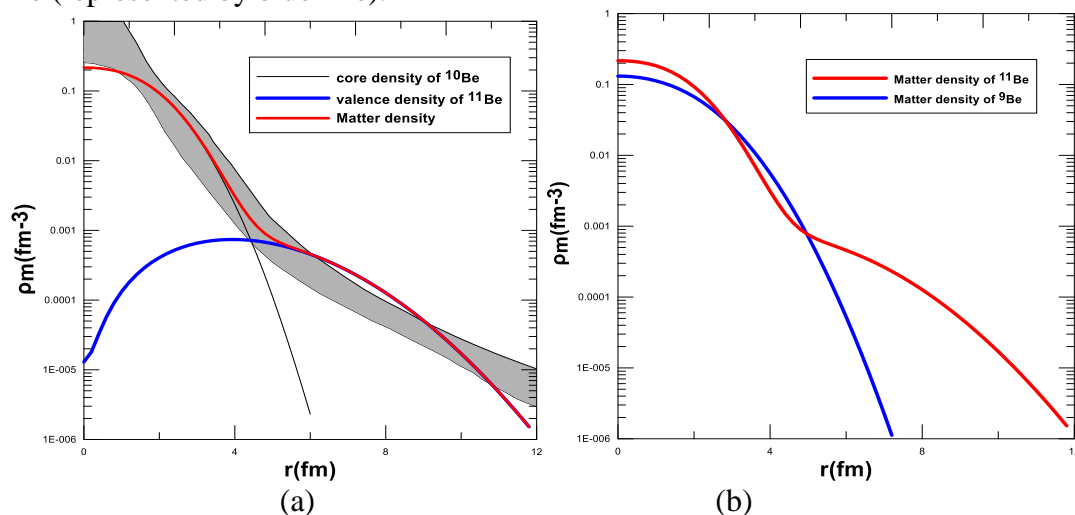
The parameters β_c and β_v used in the TFSM of the present study together with the calculated and experimental rms radii of exotic nuclei (^9C , ^{12}N , ^{23}Al , ^{11}Be , ^{15}C) are shown in Table-1. The nuclear properties which include nucleons matter density, elastic electron scattering form factor and rms radii were programmed by Fortran 90 power station.

Table 1-The Parameters β_c and β_v used in the TFSM of the present study together with the calculated and experimental rms radii of (^{11}Be , ^{15}C , ^9C , ^{12}N , ^{23}Al) exotic nuclei.

Halo nuclei	Core nuclei	β_c (fm)	β_v (fm)	rms matter radii for core nuclei $\langle r^2 \rangle_{core}^{1/2}$ (fm)		rms matter radii for halo nuclei $\langle r^2 \rangle_{halo}^{1/2}$ (fm)	
				Calculated results (P. W.)	Experimental results	Calculated results (P. W.)	Experimental results
^{11}Be	^{10}Be	1.62	1.95	2.28	2.28 ± 0.02 [20]	2.80	2.86 ± 0.04 [21]
^{15}C	^{14}C	1.60	1.88	2.34	2.3 ± 0.07 [22]	2.78	2.783 ± 0.092 [22]
^9C	^8B	1.75	2.00	2.34	2.38 ± 0.04 [22]	2.75	2.75 ± 0.34 [28]
^{12}N	^{11}C	1.52	1.70	2.18	2.18 ± 0.26 [28]	2.47	2.49 ± 0.24 [28]
^{23}Al	^{22}Mg	1.78	1.87	2.75	2.78 ± 0.26 [29]	2.92	2.905 ± 0.25 [30]

One neutron exotic nuclei:**1. ^{11}Be nucleus.**

^{11}Be ($J^\pi, T = 1/2^-, 3/2$) is formed by coupling the core ^{10}Be ($J^\pi, T = 0^+, 1$) with the valence (halo) neutron ($J^\pi, T = 1/2^-, 1/2$). The value of oscillator size parameter β_c for core (^{10}Be) is equal to 1.62fm, which gives rms nucleon radii equal to (2.28fm), while the one-neutron exotic nuclei ^{11}Be assumed to be in a pure (1p $_{1/2}$) with occupation number equal to 0.25 and oscillator size parameter $\beta_v=1.95\text{fm}$ were used to give rms nucleon radii equal to (2.80fm). These results of rms nucleon radii were obtained via calculating the matter density distribution and there was a good agreement between the theoretical results and experimental data as shown in Table-1. The two body nucleon density distribution (2BNDD) (in fm^{-3}) of the ground state was plotted against r (in fm) of the ground state, as shown in Figure 1. The black line of Figure (1-a) represents the normal contribution of core ^{10}Be , the valence (one-neutron exotic nuclei in the state of 1p $_{1/2}$) is defined by the blue line, which has a long tail, and the matter density distribution (core + valence) is represented by the red line, which also has a long tail and has a good agreement with the experimental data of Fukuda et al.[16] for ^{11}Be represented by the shaded space. Figure (1-b) shows a comparison of matter density distribution of ^{11}Be (represented by red line) and the matter density distribution of stable nuclei ^9Be (represented by blue line).

**Figure 1-** (a) Comparison of matter density distribution of ^{11}Be with that of the experimental data. (b) Comparison of matter density distribution of exotic nuclei ^{11}Be with that of stable nuclei ^9Be .

Elastic electron scattering form factors of 2BNDD are shown in Figure 2, the filled circle symbol represents the experimental data of Glickman et al.[17] for ${}^9\text{Be}$. The red line curve represents form factors with oscillator size parameter $\beta = 2.78\text{fm}$ (β assumed to be the average of β_c and β_v). Through comparing the theoretical results of the elastic electron scattering form factors for ${}^{11}\text{Be}$ nucleus with experimental data of stable ${}^9\text{Be}$ nucleus, the difference in behavior of first diffraction minimum at $q \approx 1.1\text{fm}^{-1}$ for ${}^{11}\text{Be}$ nucleus was noted.

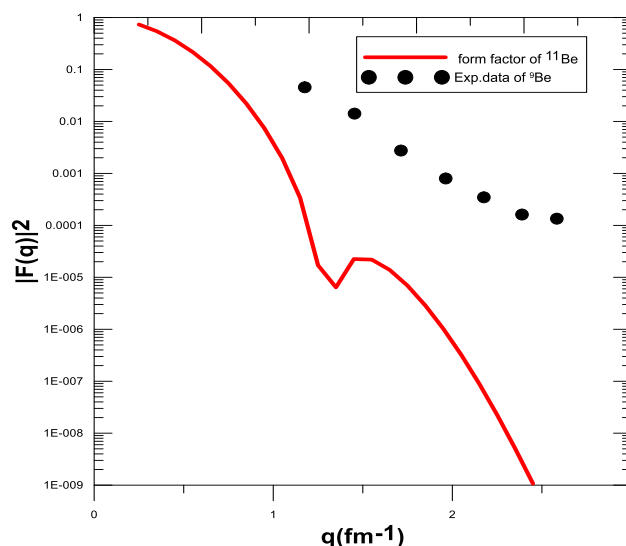


Figure 2-Comparison of measured elastic electron form factors for ${}^{11}\text{Be}$ with experimental data from Glickman et al. [17].

2. ${}^{15}\text{C}$ Nucleus:

${}^{15}\text{C}$ ($J^\pi, T = 1/2^+, 3/2$) is formed by coupling the core ${}^{14}\text{C}$ ($J^\pi, T = 0^+, 1$) with the valence one- neutron ($J^\pi, T = 1/2^+, 1/2$). A value of oscillator size parameter for core ${}^{14}\text{C}$ is equal to $\beta_c = 1.60\text{fm}$, which gives rms nucleon radii equal to (2.34fm), while the one-neutron exotic nuclei ${}^{15}\text{C}$ which is in a pure ($1d_{5/2}$) with occupation number equal to 0.083 and oscillator size parameter $\beta_v = 1.88\text{fm}$ used to give rms nucleon radii equal to 2.78fm. These results of rms nucleon radii were obtained via calculating matter density distribution. Good agreement between the theoretical results and experimental data were noted, as shown in Table-1. The two body nucleon density distribution (2BNDD) in fm^{-3} of the ground state was plotted versus r in (fm) of the ground state (Figure 3). In Figure (3-a), the black line represents the normal contribution of core ${}^{14}\text{C}$, the valence (one-neutron exotic nuclei in the state of $1d_{5/2}$) is defined by the blue line, which has a long tail and the matter density distribution (core + valence) is represented by the red line, which also has a long tail and a good agreement with the experimental data of Fang, et al. [18] for ${}^{15}\text{C}$ and represented by the shaded region. Figure (3-b) shows a comparison of matter density distribution of ${}^{15}\text{C}$ (represented by red line) with matter density distribution of ${}^{12}\text{C}$ (represented by blue line).

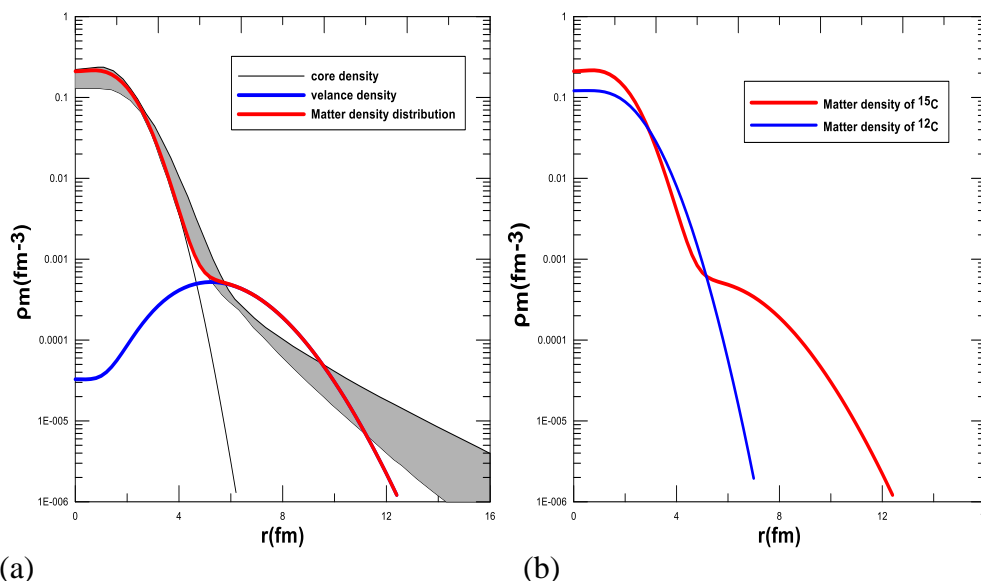


Figure 3-(a)Comparison of calculated matter density distribution with that of the experimental data for ^{15}C . (b)Comparison of matter density of exotic nuclei ^{15}C with that of stable nuclei ^{12}C .

The elastic electron scattering form factors of 2BCDD are shown in Figure 4, the red line curve represents the form factors with oscillator size parameter $\beta=2.68\text{fm}$ (β assumed to be the average of β_c and β_v), while the filled circle symbol represents the experimental data for ^{12}C taken from Crannell [19]. When the theoretical elastic electron scattering form factors for the ^{15}C nucleus were compared to experimental results for the stable nucleus ^{12}C , it was found that they behave similarly in the first diffraction minimum for ^{15}C at $q \approx 1.1\text{fm}^{-1}$ and ^{12}C at $q \approx 1.7\text{fm}^{-1}$ for ^{12}C .

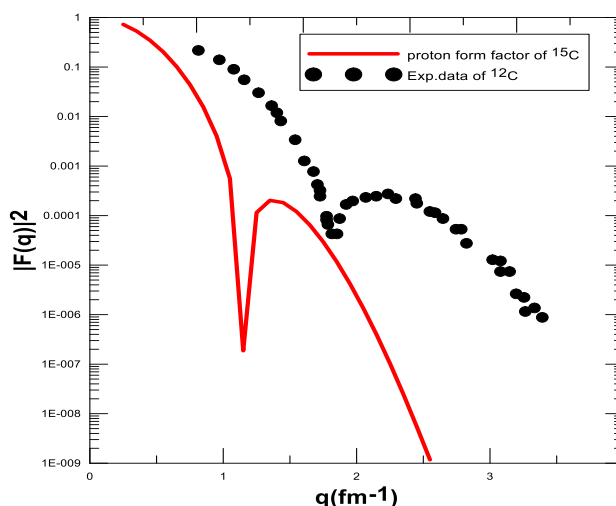


Figure 4- Comparison of the elastic electron scattering form factors of ^{15}C with experimental data of ^{12}C [19].

One proton exotic nuclei:

1. ^9C Nucleus

^9C ($J^\pi, T = 3/2^-, 3/2$) is formed by coupling the core ^8B ($J^\pi, T = 2^+, 1$) with the valence one-proton ($J^\pi, T = 1/2, 1/2$). A value of oscillator size parameter for core ^8B ($\beta_c = 1.75\text{fm}$) gives the rms nucleon radii equal to 2.34fm , while the valence one-proton exotic nuclei ^9C is to be in a pure ($1p_{1/2}$) with occupation probabilities 0.25 and oscillator size

parameter (β_v) equal to 2.00 fm to give rms nucleon radii equal to (2.75 fm). These results of rms nucleon radii were obtained via calculating the matter density distribution. The theoretical results showed good agreement with the experimental data, as shown in Table 1. The two body nucleon density distribution (2BNDD)(in fm^{-3}) was plotted versus r (fm) in the ground state(Figure 5). In Figure (5-a), the black line represents the normal contribution of core ^8B ,the valance (one-proton exotic nuclei in the state of $1P_{1/2}$) is represented by the blue line, which has a long tail and the matter density distribution of (core +valence) is represented by the red line, which also has a long tail and has a good agreement with the ^9C experimental data of ^9C of Hong et al. [20-23] which is represented by the filled circle symbol. Figure (5-b) shows the comparison between the matter density distribution of ^9C nucleus (represented by red line) and matter density distribution of stable ^{12}C nucleus (represented by the blue line).

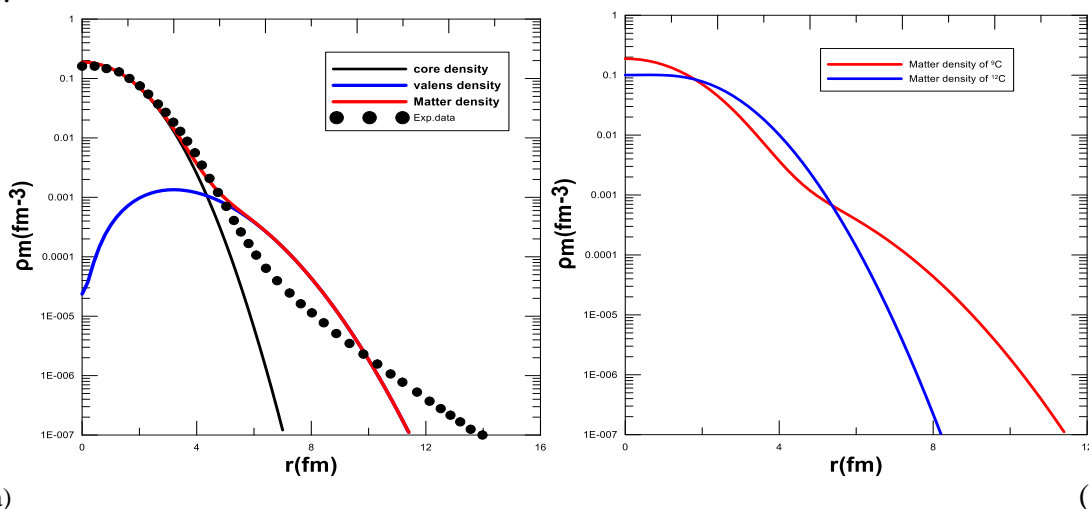


Figure 5- (a) Comparison of matter density distribution with that of the experimental data for ^9C . (b) Comparison of the matter density of exotic nuclei ^9C with that of stable nuclei ^{12}C .

The elastic electron scattering form factors of 2BNDD are shown in Figure 6, the red line curve represents the form factors with oscillator size parameter $\beta=1.87\text{fm}$ (β assumed to be the average of β_c and β_v), while the filled circle symbol represents the experiment data for ^{12}C of Crannell [19]. Through comparing the theoretical results of the elastic scattering form factors for ^9C nucleus, it was noticed that they have the same behavior of the experimental results of stable nucleus ^{12}C , but the first diffraction minimum for ^9C was at $q \approx 2.3\text{fm}^{-1}$ and for ^{12}C at $q \approx 1.8\text{fm}^{-1}$.

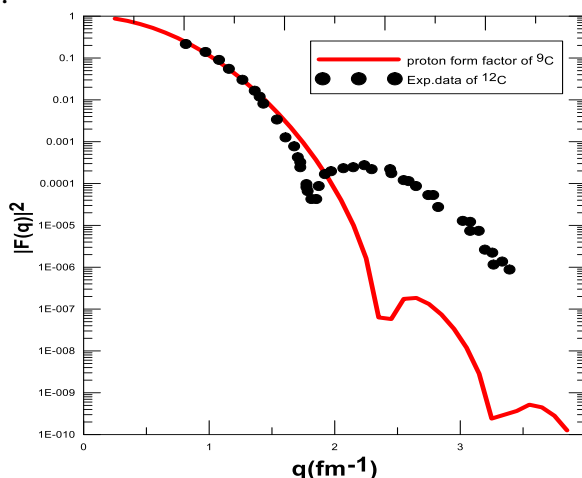


Figure 6-Comparison of the elastic electron scattering form factors of ^9C with experimental data of ^{12}C [19].

2. ^{12}N Nucleus

^{12}N ($J^\pi, T = 1^+, 1$) is formed by coupling the core ^{11}C ($J^\pi, T = 3/2^-, 1/2$) with valence one-proton ($J^\pi, T = 1/2^-, 1/2$). A value of oscillator size parameter for core ^{11}C is equal to ($\beta_c=1.52\text{fm}$) and gives rms radii equal to (2.18fm), while the valence one-proton be in pure ($1p_{1/2}$) with occupation number equal to (0.25) and oscillator size parameter equal to $\beta_v=1.70\text{fm}$ which gives rms radii equal to (2.47fm). These results of rms nucleon radii were obtained via calculating the matter density distribution. The theoretical results have a good agreement with experimental data as shown in Table 1. The two body nucleon density distribution (2BNDD) in fm^{-3} of the ground state was plotted versus r (fm) in the ground state (Figure 7). In Figure(7-a), the black line represents the normal contribution of core ^{11}C , the blue line represents the valence (one-proton exotic nuclei in state of $1p_{1/2}$) through this distribution it takes the form of a long tail, the red line represents the matter density distribution (core +valence) which takes the form of a long tail too and has a good agreement with the experimental data of ^{12}N of Xing et al. [24] which is represented by the filled circle symbol. Figure (7-b) shows a comparison of matter density distribution of ^{12}N (represented by red line) with the matter density distribution of ^{14}N (represented by the blue line).

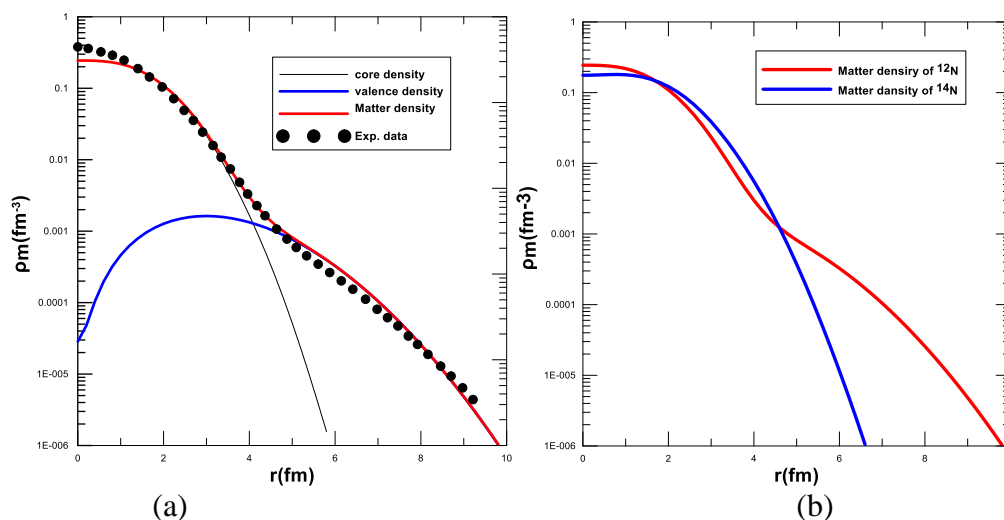


Figure 7- (a) Comparison between matter density distribution and that of the experimental data for ^{12}N . (b) Comparison between matter density of exotic nuclei ^{12}N nuclei with that of stable nuclei ^{14}N .

The elastic electron scattering form factors 2BCDD are shown in Figure 8, where the red line curve represents form factors with oscillator size parameter $\beta=1.61\text{fm}$ (β assumed to be the average of β_c and β_v), while the filled circle symbol represents the experimental data for ^{12}N of Dally et al.[25]. Through comparing the theoretical results of the elastic electron scattering form factors for ^{12}N nucleus, it was noted that they have the same behavior of the experimental results of stable nucleus ^{14}N , but the first diffraction minimum for ^{12}N was at $q \approx 2.0\text{fm}^{-1}$ and for ^{14}N at $q \approx 1.7\text{fm}^{-1}$.

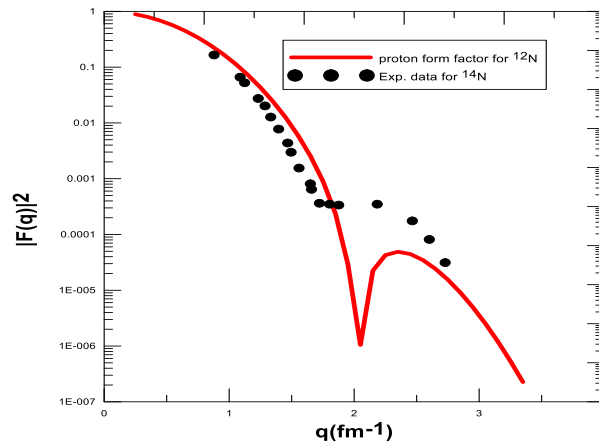


Figure 8-Comparison between elastic electron scattering form factors of ^{12}N and experimental data of ^{14}N .

3. ^{23}Al Nucleus

^{23}Al ($J^\pi, T = 1/2^+, 3/2$) is formed by coupling of the core ^{22}Mg ($J^\pi, T = 0^+, 1$) with valence one-proton ($J^\pi, T = 1/2^+, 1/2$). A value of the oscillator size parameter of core ^{22}Mg is equal to ($\beta_c=1.78\text{fm}$) and it gives rms radii equal to (2.75fm), while valence one-proton be in pure ($2s_{1/2}$) with occupation number equal to 0.25 and oscillator size parameter β_v equal to 1.87fm, which gives rms radii equal to (2.92fm). These results of rms nucleon radii were obtained via calculating the matter density distribution. There was a good agreement between the theoretical results and the experimental data. The two body nucleon density distribution (2BNDD) in fm^{-3} of the ground state was plotted versus r (fm) in the ground state (Figure 9). In Figure (9-a), the black line represents the normal contribution of core ^{22}Mg , the valence (one-proton exotic nuclei in state $2s_{1/2}$) is represented by the blue line, which has a long tail, the matter density distribution (core + valence) is represented by the red line, which also has a long tail and has a good agreement with the experimental data of Fang et al.[26] which is represented by the shaded space. Figure (9-b) represents the comparison between the matter density distribution of ^{23}Al (the red line) and the matter density distribution of ^{27}Al (the blue line).

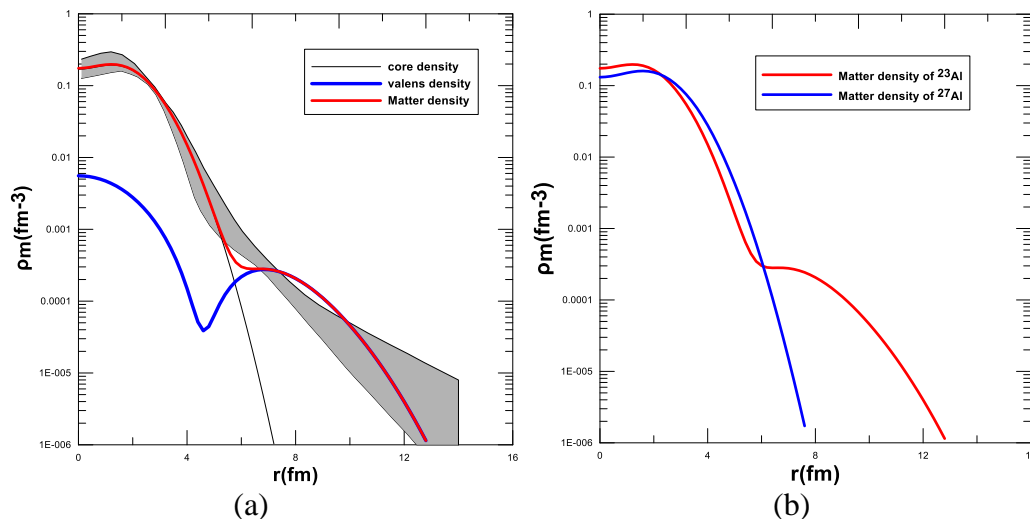


Figure 9-(a) Comparison between the matter density distribution for ^{23}Al with that of experimental data. (b): Comparison between matter density of ^{23}Al nuclei with that of ^{27}Al nuclei.

The elastic electron scattering form factors for 2BCDD are shown in Figure 10, where the red line curve represents the form factors with oscillator size parameter $\beta=1.83\text{fm}$ (β assumed to be the average of β_c and β_v), filled circle symbol represents the experimental data for ^{23}Al of Li et al.[27-30]. Through the comparison of the theoretical results of the elastic scattering form factors for nucleus ^{23}Al with the experimental results of stable nucleus ^{27}Al , it was found that they behave similarly. However, the first diffraction minimum for ^{23}Al was at $q \approx 1.5 \text{ fm}^{-1}$ and for ^{27}Al at $q \approx 1.4 \text{ fm}^{-1}$.

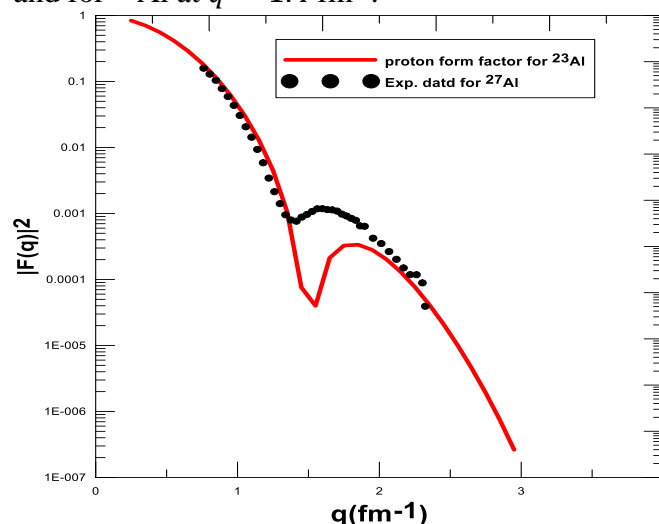


Figure 10-Comparison between the elastic electron scattering form factors of ^{23}Al and experimental data of ^{27}Al [27]

Conclusions

Because of neutron valence or proton valence, which are considered to be a distinctive characteristic of halo nuclei; in this work, the measured matter density via the framework of two body nucleon density distribution (2BNDD) with effect of tensor force (TC) and two different oscillator size parameters β_c and β_v for our exotic nuclei displayed a long tail at ($r > 6\text{fm}$) behavior. The measured matter density and rms radii of (^9C , ^{12}N , ^{23}Al , ^{11}Be , ^{15}C) exotic nuclei agreed well with the experimental results. The elastic electron scattering form factors of one-proton exotic nuclei (^9C , ^{12}N , ^{23}Al) have a similar behavior through the comparison with experimental results of stable nuclei (^{12}C , ^{14}N , ^{27}Al).

Reference

- [1] D. Lee, "Study of Nuclear Reactions with ^{11}C and ^{15}O Radioactive Ion Beams", Ph.D. thesis, *University of California, Berkeley*, 2007.
- [2] I. Tanihata, H. Hamagaki, O. Hashimoto, Y. Shida, N. Yoshikawa, K. Sugimoto, O. Yamakawa, T. Kobayashi, and N. Takahashi, "Measurements of Interaction Cross Sections and Nuclear Radii in the Light p-Shell Region", *Phys. Rev. Lett.* 55: 2676, 1985.
- [3] Gudveen Sawhney, Raj K. Gupta and Manoj K. Sharma "Importance of Deformations in Dynamical Evolution of Proton-Halo Nuclei". *Acta Physica Polonica B*, 47(3): 959, 2016.
- [4] Tanihata, I., Savajols, H. and Kanungo, R. "Recent experimental progress in nuclear halo structure studies". *Progress in Particle and Nuclear Physics*, 68: 215–313, 2013.
- [5] Takaharu Otsuka, . "Exotic nuclei and nuclear forces", *Phys. Scr.* (T152): 014007, 2013.
- [6] Adel K. Hamoudi, Gaith N. Flaiyh, Ahmed N. Abdullah, "Study of Density Distributions, Elastic Electron Scattering form factors and reaction cross sections of ^9C , ^{12}N and ^{23}Al exotic nuclei", *Iraqi Journal of Science*. 56(1A): 147-161, 2015.
- [7] Dellagiacomma, F., Orlandini, G. and Traini, M. "Dynamical correlations in finite nuclei: A simple method to study tensor effects". *Nuclear Physics A*, 393(1-2): 95-108, 1983.

- [8] Awad A. Ibraheem, Arwa S. Al-Hajjaji, M. El-Azab Farid, "Elastic scattering of one-proton halo nucleus ^{17}F on different mass targets using semi microscopic potentials", *Rev. mex. fis.* 65(2), 168-74, 2020.
- [9] Luay F. Sultan and Ahmed N. Abdullah . "Study of the Exotic Structure of Neutron-Rich ^{14}B and ^{17}C Nuclei Using the Binary Cluster Model", *Al-Nahrain Journal of Science ANJS.* 23 (4):35–39, 2020.
- [10] A. N. Antonov, P. E. Hodgson and I. Zh. Petkov, "Nucleon Momentum and Density Distribution in Nuclei", *Z Physik A* 297, 257–260, 1980.
- [11] Lawson, R. D. "Theory of the Nuclear Shell Model", *Clarendon (Oxford University Press), New York*, 1980.
- [12] J. Fiase, A. Hamoudi, J. M. Irvine and F. Yazici, "Effective Interactions for sd-Shell-Model Calculations", *J. Phys. G: Nucl. Phys.* 14(1), 27, 1988.
- [13] Arkan Ridha, "Elastic Electron Scattering From Unstable Neutron-Rich ^{19}C Exotic Nucleus". *Iraqi Journal of Science* 54(2), 324-332, 2013.
- [14] Benson, H. G. and Flowers, B. H. "A study of deformation in light nuclei: (I). Application to the ground state band of ^{20}Ne and to the low-energy spectrum of ^{19}F ". *Nuclear Physics A*, 126: 305-331, 1969.
- [15] Walecka, J. D. "Electron Scattering for Nuclear and Nucleon Structure". *Cambridge University Press, Cambridge*, 2001.
- [16] M. Fukuda, T. Ichihara, N. Inabe, T. Kubo, H. Kumagai, T. Nakagawa, Y. Yano, I. Tanihata, M. Adachi, K. Asahi, M. Kouguchi, M. Ishihara, H. Sagawa and S. Shimoura, "Neutron halo in ^{11}Be studied via reaction cross sections", *Physics Letters B*, 268(3-4), 339-344, 1991.
- [17] J. P. Glickman, W. Bertozzi, T. N. Buti, S. Dixit, F. W. Hersman, C. E. Hyde-Wright, M. V. Hynes, R. W. Lourie, B. E. Norum, J. J. Kelly, B. L. Berman, and D. J. Millener, "Electron scattering from", ^9Be , *Phys. Rev. C* 43: 1740, 1990.
- [18] D. Q. Fang, T. Yamaguchi, T. Zheng, A. Ozawa, M. Chiba, R. Kanungo, T. Kato, K. Morimoto, T. Ohnishi, T. Suda, Y. Yamaguchi, A. Yoshida, K. Yoshida, and I. Tanihata, "One-neutron halo structure in ^{15}C ". *Phys. Rev. C* 69: 034613, 2004.
- [19] H. Crannell, "Elastic and Inelastic Electron Scattering from ^{12}C and ^{16}O ". *Phys. Rev.* 148:1107, 1966.
- [20] J. S. Al-Khalili, J. A. Tostevin, and I. J. Thompson, "Radii of halo nuclei from cross section measurements", *Phys. Rev. C* 54 : 1843, 1996.
- [21] C. A. Bertulani and H. Sagawa., "Probing the ground-state and transition densities of halo nuclei" *Nuclear Physics A* 588(3), 667-692, 1995.
- [22] A. Ozawa, T. Suzuki, I. Tanihata, "Nuclear size and related topics", *Nuclear Physics A* 693(1-2), :32-62, 2001.
- [23] L. Z. Hong, G. Bing, L. W. Ping, B. X. Xiang, L. Gang, S. Jun, Y. S. Quan, W. B. Xiang and Z. Sheng, *Chin. Phys. Lett.* 22 :1870, 2005.
- [24] L. J. Xing, L. P. Ping, W. J. Song, H. Z. Guo, M. R. Shi, S. Z. Yu, L. Chen, C. R. Fu, X. H. Shan, X. G. Qing and G. Z. Yan, *Chinese Physics C* 34 : 452, 2010.
- [25] E. B. Dally, M. G. Croissiaux and B. Schweitz. "Scattering of High-Energy Electrons by Nitrogen-14 and -15", *Phys. Rev. C* 2: 2057, 1970.
- [26] D. Q. Fang, M. C. Wang, M. Y. Gang, C. X. Zhou, C. J. Gen, C. J. Hui, G. Wei, T. W. Dong, W. Kun, W. Y. Bin, Y. T. Zhi, Z. Chen, Z. J. Xu, S. W. Qing, *Chin. Phys. Lett.* 22 , 572, 2005.
- [27] G. C. Li, M. R. Yearian and I. Sick, "High-momentum-transfer electron scattering from ^{24}Mg , ^{27}Al , ^{28}Si , and ^{32}S ", *Phys. Rev. C* 9 :1861, 1974.
- [28] R. E. Warner, F. Carstoiu, J. A. Brown, F. D. Becchetti, D. A. Roberts B. Davids, A. Galonsky, R. M. Ronningen, M. Steiner, M. Horoi, J. J. Kolata, A. Nadasen, C. Samanta, J. Schwartzberg and K. Subotic, "Reaction and proton-removal cross sections of ^6Li , ^7Be , ^{10}B , $^{9,10,11}\text{C}$, ^{12}N , $^{13,15}\text{O}$, and ^{17}Ne on Si at 15 to 53 MeV/nucleon", *Phys. Rev. C* 74: 014605, 2006.
- [29] Y. L. Zhao, M. Z. Yu, C. B. Qiu and S. W. Qing, *Chin. Phys. Lett.* C 20 : 53, 2003.
- [30] H. Y. Zhang, W. Q. Shen, Z. Z. Ren, Y. G. Ma, W. Z. Jiang, Z. Y. Zhu, X. Z. Cai, D. Q. Fang, C. Zhong, L. P. Yu, Y. B. Wei, W. L. Zhan , Z. Y. *Chin Phys. Lett.* 22:3, 2005.